

Railway Wheel Detector in the Presence of Eddy Current Brakes

A. Zamani and A. Mirabadi

School of Railway Engineering
Iran University of Science and Technology, Tehran, Iran
alizamani.e@gmail.com and mirabadi@iust.ac.ir

Abstract — In this paper, electromagnetic sensor is considered as a train wheel detector, which is one of the most important signalling systems to determine the clearance or occupancy of a track section. The wheel detector is affected by eddy current brakes and this problem has limited its use. In order to improve the wheel detection accuracy and eliminate the eddy current brake effect, the optimal design of sensors is carried out by means of finite element method. Kriging method is utilized to reduce the computational costs. Additionally, genetic algorithm is used as a multi-objective optimization method to find the optimum orientation.

Index Terms - Eddy current brakes, finite element method, genetic algorithm, Kriging, multi-objective optimization, and train wheel detector.

I. INTRODUCTION

Train detection equipment is considered as one of the most important and critical subsystems of the entire railway signaling system, with great importance for passenger and service safety. Axle counter is a particular type of train detection system, which is used widely on many railway lines, because of its beneficial features such as ease of installation, flexibility and low cost, over other train detection systems. Axle counters usually work on the basis of electromagnetic waves. Two coils installed on either side of a rail, acting respectively as transmitter and receiver, perform the role of wheel detector or axle counter sensors as shown in Fig. 1.

The axle counter system may be affected by eddy current brakes. Eddy Current Brake (ECB) is a developing brake system which makes use of Lenz's law to stop the train without mechanical

contact. Due to the destroying effect of the ECB on the axle counter, in practice, trains with the eddy current brakes are not allowed to pass through the lines with the axle counter system. However, a wide range of studies aimed to solve such problems, which have been conducted by various researchers around the world. Different researchers, authorities, and companies have designed and developed new hardware and software [1, 2]. However, these designs cannot be implemented on old systems and also removing the old system and installing the new system is very expensive. So, a method for improving the old system is cheaper and more efficient. Experience shows that improving the orientation and position of the coils, is one of the cheapest and most effective methods in enhancing the performance of the system and improving the quality of the signal received in the receiving coil.

In order to find the optimum orientation of the coils, the authors of the present paper have studied the performance of the Response Surface Methodology (RSM) and also Kriging method in their recent publications [3, 4]. In the current paper, Kriging method and the Genetic Algorithm (GA) as a multi-objective optimization method are used to find the optimum orientation of the axle counter sensors and eliminate the ECB effect on it. Given the permanent and transient environmental noises and their effects on the sensors' performance and also the wide range of possible orientations, which can be considered, make it difficult to test all possible conditions with actual sensors. Modeling the system and simulating various local and environmental conditions provide an opportunity to analyse the system performance over a much wider range of orientations to find the optimum sensor coil orientation of the system.

In this research a finite element method (FEM) has been used to determine the induced voltage in the receiving coil. However, the FEM analysis of the whole continuous search space is time consuming and requires excessive processing effort. So the FEM analysis has been implemented for a limited number of orientations and then metamodelling techniques are utilized to estimate the performance of the system in other points of the spectrum. RSM, Kriging and MARS (Multivariate Adaptive Regression Splines) have been identified as the three most effective approaches in a range of applications, in that they provide the possibility of analysing the whole search space of the system. It is approved that Kriging method has the best performance through the other methods for the train wheel detector system [4]. Using the Kriging method provides two response surfaces, which should be optimized. Finally, a multi-objective optimizer such as genetic algorithm is needed to optimize the two response surfaces.

II. TRAIN WHEEL DETECTOR

Even in the early days of the railway in the 19th century, wheel detection had been an urgent desire for railway engineers, where they were concerned about signalling safety. In the past, mechanical, hydraulic, and finally pneumatic systems were used as a wheel detector. But, due to their limited application and deficient in high speeds, they were replaced in the 1950s by magnetic and contactless inductive devices. Today, the most common wheel detectors in Iran and many other countries are contactless inductive wheel detectors. They are easy to install, flexible, and low cost. Inductive wheel detectors make use of the electromagnetic flux linkage between two coils that are mounted on either side of the rail, to detect the passage of the wheels. Figure 1 shows a wheel detector.

Detailed analysis with the electromagnetic equations for the train wheel detector is performed in [4]. The FEM is used to determine the electromagnetic field around the sensor coils and also the induced voltage in the receiving coil. This provides the opportunity to model the system in a variety of coil orientations. Results of FEM modelling have been shown in Fig. 2. This figure illustrates the distribution of the flux lines in the presence and absence of the wheel. When there is

no wheel between receiver and transmitter coils as shown in Fig. 2 (a), the magnetic flux flows along the receiving coil and induces a voltage in it. On the other hand, in the presence of the wheel as presented in Fig. 2 (b), less magnetic flux flows along the receiving coil and hence the lower induced voltage in the receiver.

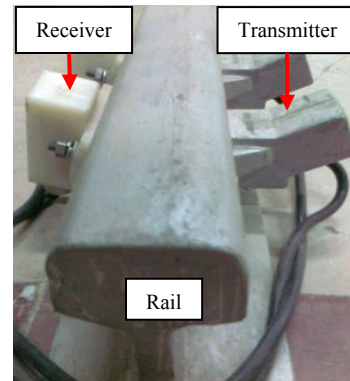


Fig. 1. Train wheel detector.

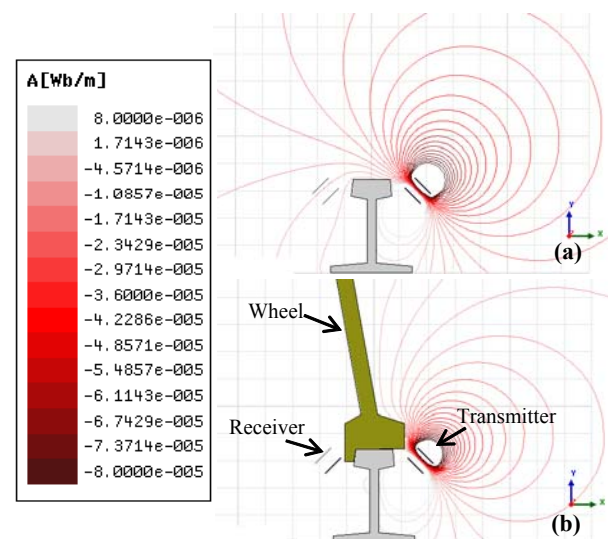


Fig. 2. Distribution of the flux lines with (a) no wheel and (b) wheel present.

In order to detect the passage of a wheel, the induced voltage in the receiving coil is monitored continuously. Furthermore, any changes exceeding predefined thresholds are interpreted as being caused by the presence or absence of a wheel. In other words, the wheel detector detects the wheel when the amplitude of the induced voltage in the receiving coil is less than a threshold level, as shown in Fig. 3.

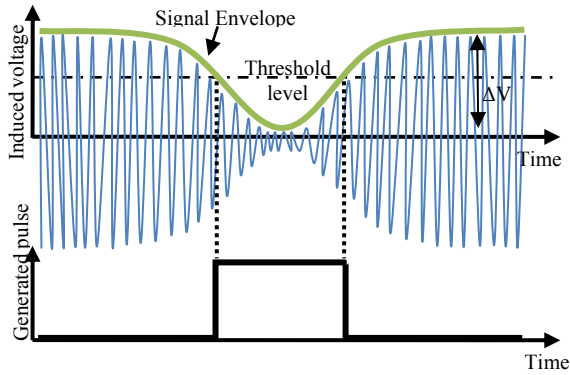


Fig. 3. Induced voltage and detecting principles.

Although axle counters are proven to be more reliable compared to other types of train detectors, it sometimes fails because of electromagnetic interferences and passage of trains with ECBs. The effect of electromagnetic noise on the output signal can be reduced or eliminated by generating a large difference in the voltage amplitudes, in the presence and absence of a wheel (ΔV). In the case which there is no ECB, the authors of the present paper have suggested $(-45^\circ, 45^\circ)$ orientation for the wheel detectors [4]. In this paper, the authors are trying to find an appropriate orientation for the wheel detector coils to solve the problem of wheel detector in the presence of eddy current brake.

III. EDDY CURRENT BRAKE

The eddy current brake consists of a magnetic yoke with electrical coils positioned along the rail, which are being magnetized alternating as south and north magnetic poles as shown in Fig. 4. This magnet does not touch the rail, but is held at a definite small distance from the rail (approximately 7 mm). It does not move along the rail, it exerts only a vertical pull on the rail [5, 6].

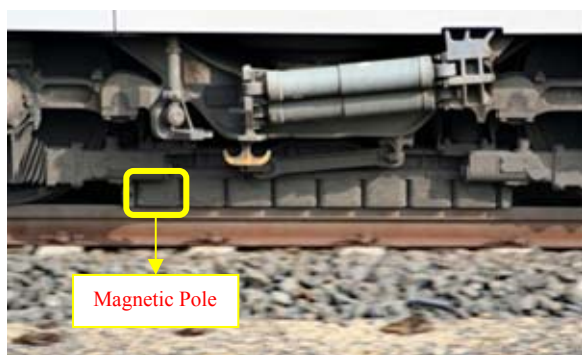


Fig. 4. Eddy current brake with 8 poles.

An ECB can affect the wheel detector in two possible ways: first, the ECB can affect the wheel detector as the wheel does. In other words, when the brakes are placed between the coils of the wheel detector, less magnetic flux arrives to the receiving coil and hence, lower voltage will be induced in the receiver and the ECB may be detected as a wheel. The second way is the transient current, which passes through the ECB. In this way, if the brake is near the wheel detector, it may induce a disturbing voltage in the coils of the wheel detector. However, the processor unit of an axle counter system detects only changes that have more than 5 second lengths; so, transient voltages cannot affect the whole axle counter system. Therefore, in this paper only the first effect of the ECB (physical presence) is analysed.

To analyse the effect of the ECB on the wheel detector, it is modelled by the FEM as shown in Fig. 5. This figure shows the FEM model of an ECB with six poles in the presence of the wheel detector.

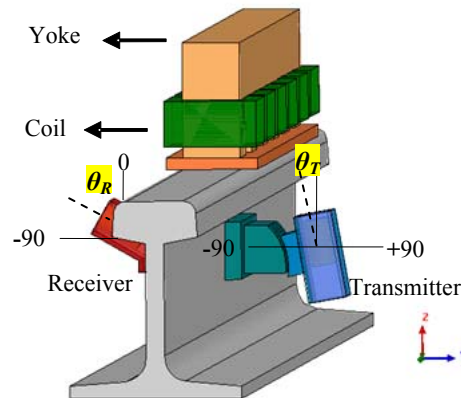


Fig. 5. FEM model of eddy current brake and wheel detector.

The distribution of the flux lines produced by the transmitter of the wheel detector, in the presence of the ECB is displayed in Fig. 6. In this figure the wheel detector coils are located in $(\theta_R, \theta_T) = (45^\circ, -45^\circ)$, in which θ_R and θ_T are the receiver and transmitter angles, respectively. As can be seen from Fig. 6, the presence of the ECB between the coils causes reduction in the flux lines near the receiver. This reduction subsequently causes falling in the induced voltage in the receiver. This figure should be compared with Fig. 2, which displays the distribution of flux in the

presence and absence of the wheel. It can be comprehended that the effect of the ECB is very similar to that of the wheel.

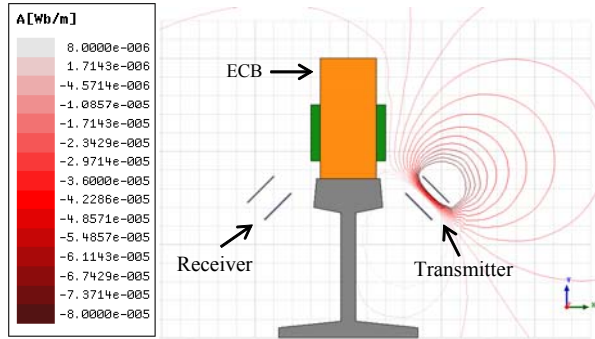


Fig. 6. Distribution of the flux lines in the presence of the eddy current brake.

The results of the FEM modeling show that the induced voltage in the presence of the ECB is about 230 mV, which is lower than the threshold level (470 mV), and consequently, the brake is recognized as a wheel. This status is indicated in Fig. 7.

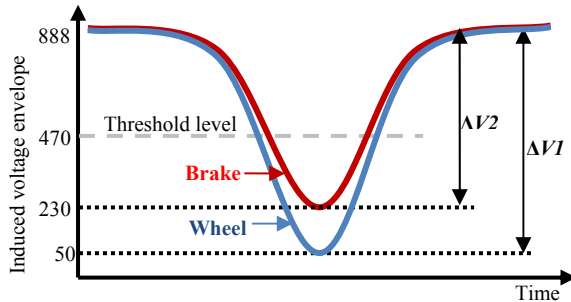


Fig. 7. Induced voltage envelopes by passing the wheel and the eddy current brake when coils are positioned in $(\theta_R, \theta_T) = (-45^\circ, 45^\circ)$.

To solve this problem, the coils should be located in the optimized orientation in which the induced voltage envelope by passing the wheel is lower than the threshold level. Simultaneously, this voltage should be more than the threshold level by the passage of the brake. For this purpose the induced voltage for three situations: 1) without wheel and brake, 2) with wheel and with brake, and 3) in all orientations should be calculated. It can be easily comprehended that the voltage calculation for the all possible ranges of θ_R and θ_T

(-90 to +90 degrees) is impossible. Therefore, a metamodeling technique like Kriging, which can almost accurately estimate the full-range voltages, is needed.

Using the Kriging method, two response surfaces (i.e., objectives) will be created. The first objective is for the voltage difference between the wheel absence and presence, which is indicated by ΔV_1 in Fig. 7, which should be maximized. The second objective is for the voltage difference between the brake absence and presence, which is illustrated by ΔV_2 in Fig. 7, and should be minimized. To find the optimum orientation in which both of the mentioned requirements are fulfilled, a multi-objective optimization method should be used. Both, Kriging method and multi-objective optimization method are explained in the following section.

IV. OPTIMIZATION

The aim of optimizing the wheel detector design, as an electromagnetic system, is to determine the most appropriate orientation of the coils, to achieve the following three goals:

- 1- Maximum sensitivity in detecting the train wheels,
- 2- maximum protection against the electromagnetic noises,
- 3- avoid detecting the ECB as a wheel.

The first and second goals mean that ΔV_1 should be maximized, and the third goal means that ΔV_2 should be minimized. In other words, the aim of the optimization is to find the set of optimum θ_R and θ_T values, which provide the maximum ΔV_1 and at the same time the minimum ΔV_2 . Thus, the system can be recognized as a “two inputs – two outputs” system, in which θ_R and θ_T are the inputs and ΔV_1 and ΔV_2 are the outputs. However, finding functions for $\Delta V_1(\theta_R, \theta_T)$ and $\Delta V_2(\theta_R, \theta_T)$ is not possible, but using statistical approximate models, such as Kriging model are recommended in some engineering cases [7, 8]. Although these approaches are not as accurate as direct optimization methods, they can be categorized as fast methods. A short explanation on the Kriging method is represented as follows.

A. Kriging method

Kriging, also called spatial modeling, is a regression method that is becoming more popular in optimization algorithms due to its advantages in

modeling nonlinear surfaces [9]. The Kriging model is defined as follows,

$$y(x) = f(x) + Z(x) \quad (1)$$

where $f(x)$ is the known approximation function, which is usually taken as a constant β and $Z(x)$ is the realization of a stochastic process with mean zero, variance σ^2 , and covariance C .

The covariance matrix $C = [c_{ij}]$ can be defined as,

$$c_{ij} = \sigma^2 \mathbf{R}[R(x_i, x_j)], \quad i, j = 1, 2, \dots, n \quad (2)$$

where \mathbf{R} is the correlation matrix and R is the user specified correlation functions. A popular choice for the correlation function is

$$R(x_i, x_j) = \prod_{k=1}^m \exp(-\alpha_k |x_i - x_j|^2), \quad (3)$$

where m is the number of design variables and α_k represents the unknown correlation function parameter vector. Small values of α_k smoothen the Kriging prediction, while for large values of α_k the Kriging model has accurate predictions around the sampled points over which it is built, and false predictions elsewhere.

Estimation of the response $y(x)$ at untried values of x is given by $\hat{y}(x)$

$$\hat{y} = \hat{\beta} + r^T(x) \mathbf{R}^{-1} (y - f\hat{\beta}), \quad (4)$$

where f is an $n \times 1$ vector of ones, when $f(x)$ is taken as constant, then $r^T(x)$ is the correlation between x and n sample points is expressed by,

$$r^T(x) = [R(x, x_1), R(x, x_2), \dots, R(x, x_n)]^T \quad (5)$$

and $\hat{\beta}$ is an estimation of β , which is

$$\hat{\beta} = (f^T \mathbf{R}^{-1} f)^{-1} (f^T \mathbf{R}^{-1} y). \quad (6)$$

The above estimation is the minimum variance linear unbiased estimation, which is an optimal estimation in the statistical sense [10].

The estimated variance, $\hat{\sigma}^2$, is obtained from,

$$\hat{\sigma}^2 = \frac{1}{n} [(y - f\hat{\beta})^T \mathbf{R}^{-1} (y - f\hat{\beta})]. \quad (7)$$

The maximum likelihood estimator of α is then obtained by maximizing

$$\Phi(\alpha) = -\frac{1}{2} (n \ln(\hat{\sigma}^2) + \ln(|\mathbf{R}|)). \quad (8)$$

Both $\hat{\sigma}^2$ and $|\mathbf{R}|$ are functions of α and the solution of this nonlinear problem gives us the value of α and allows us to evaluate the function with the best linear unbiased estimation of β .

Using the explained method for ΔV_1 and ΔV_2 with 64 experimental points generated the two response surfaces are shown in Fig. 8.

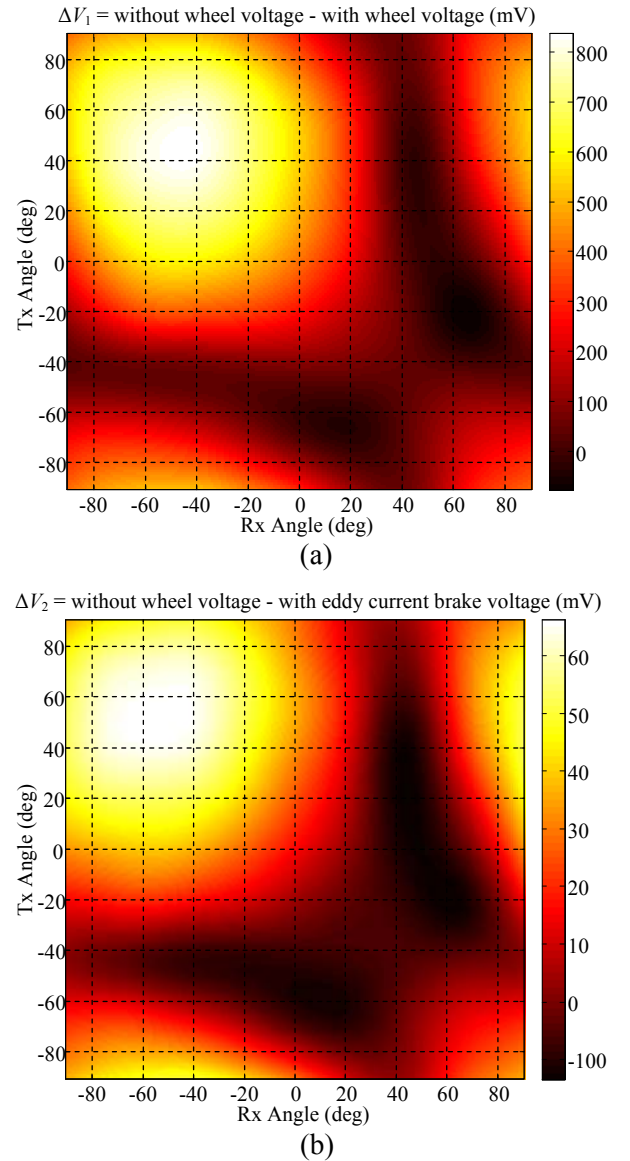


Fig. 8. (a) ΔV_1 and (b) ΔV_2 both, versus angles of receiver and transmitter coils.

B. Multi-objective optimization

Finding an optimum point for systems by more than one objective is not as easy as for one-objective systems, especially when improvement in one objective requires degradation in the other objectives. In this paper there are two variables (θ_R and θ_T), and two objectives (ΔV_1 and ΔV_2). So a system with two inputs and two outputs should be considered.

Assume a system with two variables (i.e., inputs) x_1 and x_2 in the parameter space Ω , and two objectives (i.e., outputs) F_1 and F_2 in the objective function space Λ ,

$$\Omega = \{x \in R^2\} \quad (9)$$

$$\Lambda = \{y \in R^2 : y = F(x), x \in \Omega\}. \quad (10)$$

The performance vector $F(x)$ maps the parameter space into the two dimension objective function space, shown in Fig. 9.

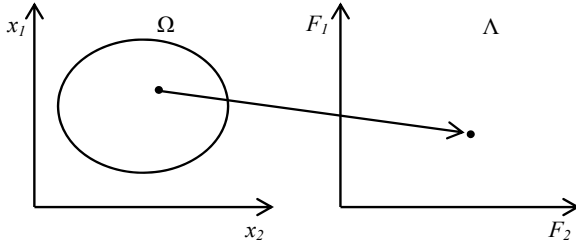


Fig. 9. Mapping from parameter space into objective function space.

The purpose is finding a non-inferior solution, which simultaneously minimizes F_1 and F_2 [11]. For this purpose, the objectives F_1 and F_2 must be traded off. A two dimensional representation is shown in Fig. 10, where the set of non-inferior solutions lie on the curve between A and B .

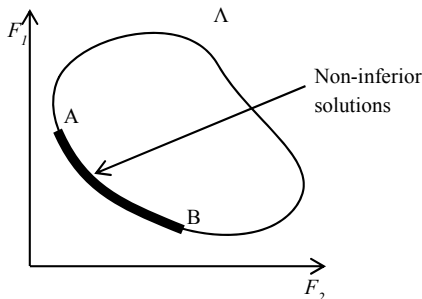


Fig. 10. Set of non-inferior solutions.

It can be clearly seen from Fig. 10 that an improvement in one objective, F_1 , requires degradation in the other objective, F_2 . So any points on the curve between A and B are non-inferior solution points. Since any point in Ω that is an inferior point that represents a point in which improvement can be attained in all the objectives, it is clear that such a point is of no value. Multi-objective optimization is, therefore, concerned with the generation and selection of non-inferior solution points [12].

There are several algorithms to find the non-inferior points in a multi-objective optimization problem. The most popular, easiest to implement, and most efficient one is the Non-dominated Sorting Genetic Algorithm II (NSGA-II) [13]. This algorithm sorts the current population according to the amount of solutions that dominate each other individual. A solution x_i is said to dominate the other solution y_i , if both of the following conditions are true,

1. $f_j(x_i) \leq f_j(y_i)$ for all functions j ,
2. $f_j(x_i) < f_j(y_i)$ for at least one function j .

At any generation, an offspring population Q is first created from the parent population P with the usual crossover and mutation operators from GA. Thereafter, the number of solutions y_i that dominate the current solution x_i is counted. This is done for all individuals from both the parent population P and the offspring population Q . Some solutions will be found to be zero when other solutions dominate them. They are non-dominated, and thus are part of the Pareto front of the current populations. The solutions that have only one other solution dominate them, would have been part of the Pareto front if the members forming the true Pareto front would not have been present. Those who have two solutions dominating them would have formed the Pareto front if those solutions would have not been present, etc. Thus, the level of domination is indicative of the quality of that solution.

Next, the crowding distances are computed. These are the average distances between one solution and its surrounding solutions in the function-value space. Then, a new population R , which contains individuals from the previous two populations P and Q , sorted by their level of dominance, will be created. That is, first insert all Pareto members in R , and then insert those that have only one dominating solution, etc. Keep inserting individuals until R is the same size as P and Q . After that, a subset P_{i+1} from R by a binary tournament selection is created. This selection takes two random individuals from R , a_R and b_R , and lets them compete using their domination level and crowding distances as competitive factors. The "winning" individual is the one that satisfies the following: 1) rank (a) < rank (b) or 2) [rank (a) = rank (b) and the crowding distance (a)

> the crowding distance (b)]. Finally, a new offspring population Q_{i+1} is created, which is equal in size to the original P , Q , and R , using crossover and mutation from GA, using members from the subset P_{i+1} as parents. After the initialization step, the rest of the steps are then repeated.

In this paper the purpose is to find θ_R and θ_T values, which provide the maximum ΔV_1 (or the minimum “ $-\Delta V_1$ ”) and at the same time the minimum ΔV_2 . NSGA-II runs with a population size of 50 and for 50 generations. The variables are used as real numbers and a recombination operator with crossover probability of $p_c = 0.9$, distribution index of $\eta_c = 10$, a polynomial mutation operator with mutation probability of $p_m = 0.5$, and finally, a distribution index of $\eta_m = 15$ are used. The result is shown in Fig. 11. The optimum response is calculated as $(\theta_R, \theta_T) = (-7^\circ, 5^\circ)$, in which ΔV_1 and ΔV_2 are, respectively, 485 and 227 mV.

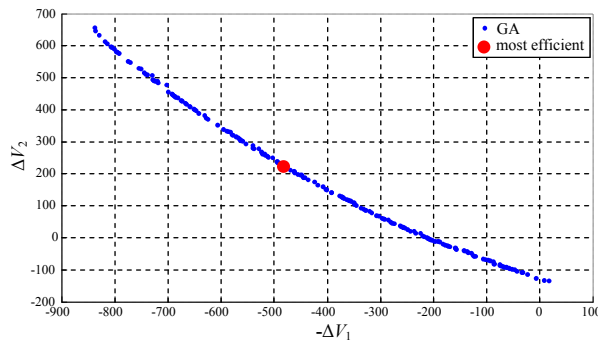


Fig. 11. Non-inferior solutions produced by GA.

V. RESULTS AND ANALYSIS

By locating the sensors in the optimum orientation, $(\theta_R, \theta_T) = (-7^\circ, 5^\circ)$, the induced voltage envelopes by passing the wheel and the ECB will change as shown in Fig. 12. The new calculated orientation and the former are compared in Table 1. Difference between ΔV_1 and ΔV_2 is calculated to reveal the amount of success in the reduction of the brake effect on the wheel detector. In fact, a great ΔV_1 and a small ΔV_2 is the goal; so, the greater “ $\Delta V_1 - \Delta V_2$ ” means the better solution.

It can be seen from this table that both of, ΔV_1 and ΔV_2 are reduced in the new orientation, but reduction in ΔV_2 is more considerable and thus “ $\Delta V_1 - \Delta V_2$ ” is improved. It means that in this orientation, the brake will not substantially affect

the induced voltage and will not be detected as a wheel. Although in the new orientation ΔV_1 is lessened from 838 mV in $(-45^\circ, 45^\circ)$ to 485 mV, the system sensitivity of the wheel is adequate. This is because the processing unit is able to sense voltages in the range of hundreds of millivolts and the output pulse will thus be generated by the passage of the wheel. In addition, the ECB will not be recognized as a wheel, because the induced voltage in the receiver is less than the threshold level. However, the threshold level should be adjusted again. As it is shown in Fig. 12, the threshold level is adjusted to the center of ΔV_1 , which is 383 mV. Therefore, the processing unit will generate a pulse by the passage of a wheel, but the ECB will not affect the processing unit.

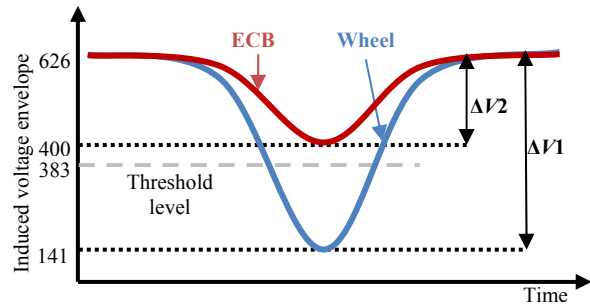


Fig. 12. Induced voltage envelopes by passing the wheel and the eddy current brake when coils are positioned in $(\theta_R, \theta_T) = (-7^\circ, 5^\circ)$.

Table 1: Comparison of different orientations.

Orientation	$(-45^\circ, 45^\circ)$	$(-7^\circ, 5^\circ)$
Voltage (mV)		
ΔV_1	838	485
ΔV_2	658	227
$\Delta V_1 - \Delta V_2$	180	258

VI. CONCLUSION

The aim of this paper was to eliminate the effect of eddy current brake on the train wheel detector without degradation of its performance against electromagnetic noises and its sensitivity to train wheels. Due to the fact that sensor orientation has a great effect on the amplitude of the induced voltage at the receiving coil, the authors focused on it. Kriging method was used for mathematical modeling of the induced voltage,

which changes over coils' angles. Then, genetic algorithm was used for finding the optimum orientation from two objectives that had been obtained by Kriging method.

The analysis results, showed that coil orientations of -7° , $+5^\circ$, with the modeled constraints and conditions, present the optimum solution. However, these measurements are the results of simulation and may change in the real world. In this research the following assumptions were made: the effect of the rail vehicle body shell is neglected, and the train wheel and eddy current brake are considered to be stationary. More realistic conditions, like the influence of the vehicle body and also the wheel and eddy current brake motions, will be considered for future studies in this area.

REFERENCES

- [1] T. Haecker and R. Klemm, "Development and testing of an axle counter which is insensitive to the impacts of high-speed traction vehicles Final report," *Stuttgart*, TV8822A2, 1993.
- [2] J. Frauscher, "From track switch to inductive wheel sensor using a variety of technologies," *Signal + Draht*, vol. 1+2, no. 98, pp. 67-71, 2006.
- [3] A. Zamani and A. Mirabadi, "Analysis of sensor orientation in railway axle counters using response surface methodology," *5th SASTech*, Mashhad, pp. 1-7, 2011.
- [4] A. Zamani, A. Mirabadi, and F. Schmid, "Applying metamodeling techniques in the design and optimization of train wheel detector," *Sensor Review*, vol. 32, no. 4, pp. 327-336, 2012.
- [5] I. Tsukerman, M. Mirzayee, M. Mirsalim, and H. Gholizad, "Motional eddy currents analysis in moving solid iron using magnetic equivalent circuits' method," *IEEE Proc. of Wireless Comm. and Appl. Comp. Electro. Soc. IEEE/ACES International Conference*, pp. 533-536, 2005.
- [6] S. Kitanov and A. Podolskii, "Analysis of eddy-current and magnetic rail brakes for high-speed trains," *The Open Transportation Journal*, vol. 2, pp. 19-28, 2008.
- [7] J. P. Kleijnen, "Kriging metamodeling in simulation: A review," *European Journal of Operation Research*, vol. 192, no. 3, pp. 707-716, 2009.
- [8] S. Koziel and J. W. Bandler, "Accurate modeling of microwave devices using space mapping and Kriging," *Int. Review of Progress in Appl. Comp. Electro.*, Tampere, Finland, pp. 902-907, April 26-29, 2010.
- [9] J. Kleijnen, "Design and analysis of computational experiments: overview," *Experimental Methods for the Analysis of Optimization Algorithms*, Thomas Bartz-Beielstein et al., Eds. Berlin: Springer, pp. 51-72, 2010.
- [10] G. Lei, K. R. Shao, Y. Guo, J. Zhu, and J. D. Lavers, "Sequential optimization method for the design of electromagnetic device," *IEEE Trans. on Magnetic*, vol. 44, pp. 3217-3220, 2008.
- [11] L. A. Zadeh, "Optimality and non-scalar-valued performance criteria," *IEEE Trans. on Automation Control*, vol. 8, no. 1, pp. 59-60, 1963.
- [12] K. Deb, *Multi-Objective Optimization using Evolutionary Algorithms*. Chichester, England: John Wiley & Sons, Ltd, 2001.
- [13] K. Deb, S. Agrawal, A. Pratap, and T. Meyarivan, "A fast and elitist multi-objective genetic algorithm: NSGA-II," *IEEE Trans. on Evol. Comp.*, vol. 6, pp. 182-197, 2002.



Ali Zamani received the B.Sc. Degree in Electrical Engineering from the University of Isfahan in 2008 and the M.Sc. Degree in Electric-Railway Engineering from Iran University of Science and Technology in 2011. During his M.Sc. Program, he worked on the design and optimization of railway axle counters. His research interests include applied electromagnetic and railway signaling.



Ahamd Mirabadi received his Ph.D. Degree in Control Engineering from the University of Sheffield in 2000 and the M.Sc. Degree in Mechatronics and optical Engineering from Loughborough University in 1994. He is an Associate Professor with the School of Railway Engineering, Iran University of Science and Technology. He is an author of numerous scientific papers in the field of railway control and signaling. His research interests include railway signaling and operation simulation, railway maintenance and condition monitoring, and safety critical systems.